LETTERS

Patient-specific induced pluripotent stem-cell-derived models of LEOPARD syndrome

Xonia Carvajal-Vergara[1,2], Ana Sevilla[1]*, Sunita L. D'Souza[1]*, Yen-Sin Ang[1], Christoph Schaniel[1], Dung-Fang Lee[1], Lei Yang[1], Aaron D. Kaplan[3], Eric D. Adler[3], Roye Rozov[1], YongChao Ge[4], Ninette Cohen[5], Lisa J. Edelmann[5], Betty Chang[1], Avinash Waghray[1], Jie Su[1], Sherly Pardo[5,6], Klaske D. Lichtenbelt[7], Marco Tartaglia[8], Bruce D. Gelb[5,6,9]* & Ihor R. Lemischka[1]*

The generation of reprogrammed induced pluripotent stem cells (iPSCs) from patients with defined genetic disorders holds the promise of increased understanding of the aetiologies of complex diseases and may also facilitate the development of novel therapeutic interventions. We have generated iPSCs from patients with LEOPARD syndrome (an acronym formed from its main features; that is, lentigines, electrocardiographic abnormalities, ocular hypertelorism, pulmonary valve stenosis, abnormal genitalia, retardation of growth and deafness), an autosomal-dominant developmental disorder belonging to a relatively prevalent class of inherited RAS–mitogen-activated protein kinase signalling diseases, which also includes Noonan syndrome, with pleomorphic effects on several tissues and organ systems[1,2]. The patient-derived cells have a mutation in the *PTPN11* gene, which encodes the SHP2 phosphatase. The iPSCs have been extensively characterized and produce multiple differentiated cell lineages. A major disease phenotype in patients with LEOPARD syndrome is hypertrophic cardiomyopathy. We show that *in vitro*-derived cardiomyocytes from LEOPARD syndrome iPSCs are larger, have a higher degree of sarcomeric organization and preferential localization of NFATC4 in the nucleus when compared with cardiomyocytes derived from human embryonic stem cells or wild-type iPSCs derived from a healthy brother of one of the LEOPARD syndrome patients. These features correlate with a potential hypertrophic state. We also provide molecular insights into signalling pathways that may promote the disease phenotype.

Approximately 90% of LEOPARD syndrome cases, and 45% of Noonan syndrome cases, are caused by missense mutations in the *PTPN11* gene which encodes the protein tyrosine phosphatase SHP2. *PTPN11* is ubiquitously expressed, essential for normal development, and somatic mutations in this gene contribute to leukaemogenesis in children[3,4]. For LEOPARD syndrome, two mutations, T468M and Y279C, are most recurrent[5]. Hypertrophic cardiomyopathy is the most common life-threatening cardiac anomaly in LEOPARD syndrome[2]. Animal models of LEOPARD syndrome have been generated in *Drosophila* and zebrafish[6,7], but the molecular pathogenesis of LEOPARD syndrome remains obscure.

Ectopic expression of four transcription factors (*OCT4* (also called POU5F1), *SOX2*, *KLF4* and *MYC*) in adult human dermal fibroblasts can generate pluripotent iPSCs[8–10]. Together with defined *in vitro* differentiation protocols, this suggests the possibility of developing reliable disease models[11–14]. We have established iPSC lines from two LEOPARD syndrome patients, a 25-year-old female (L1) and a 34-year-old male (L2). A heterozygous T468M substitution mutation in *PTPN11* is present in both.

Fibroblasts were transduced with *OCT4*-, *SOX2*-, *KLF4*- and *MYC*-encoding VSV-pseudotyped Moloney-based retroviral vectors. Compact embryonic stem (ES)-cell-like colonies emerged after 2 weeks and TRA1-81-positive colonies were clonally expanded to create stable LEOPARD syndrome iPSC lines (Supplementary Fig. 1)[8]. Three iPSC lines per patient were used for preliminary characterization: L1-iPS1, L1-iPS6, L1-iPS13, L2-iPS6, L2-iPS16 and L2-iPS18.

To verify that the iPSCs originated from patient-derived fibroblasts, we performed DNA fingerprinting analysis (Supplementary Fig. 2a). All iPSCs had normal karyotypes of 46,XX (L1) and 46,XY (L2) (Supplementary Fig. 2b and data not shown). In addition, they carried the expected T468M mutation (Supplementary Fig. 3a). Restriction fragment length polymorphism analysis of a polymerase chain reaction with reverse transcription (RT–PCR) amplimer containing the mutation with BsmFI showed biallelic expression of *PTPN11* (Supplementary Fig. 3b). PCR and Southern blot analysis indicated the presence of all four transgene proviruses in the LEOPARD syndrome iPSCs (Supplementary Fig. 4), and quantitative RT–PCR (qRT–PCR) results confirmed efficient transgene silencing (Supplementary Fig. 5).

To characterize further the LEOPARD syndrome iPSC clones, expression of several human ES-cell markers in two LEOPARD syndrome iPSC lines from each patient (L1-iPS1, L1-iPS13, L2-iPS6 and L2-iPS16) was analysed and compared to the HES2 human ES cell line and a wild-type iPSC line, BJ-iPSB5, derived in our laboratory from a normal human fibroblast line (BJ). The BJ-iPSB5 cell line was also karyotypically normal (46,XY), and contained all four transgene proviruses, which were silenced (Supplementary Figs 2b, 4b and 5b). All LEOPARD syndrome and control iPSC lines showed high alkaline phosphatase activity and expressed pluripotency markers, including surface antigens TRA1-81, TRA1-60 and SSEA4, as well as the nuclear transcription factors OCT4 and NANOG (Supplementary Fig. 6). Activation of a series of endogenous stemness genes (*OCT4*, *NANOG*, *SOX2*, *GDF3*, *DPPA4*, *REX1* and *TERT*) in iPSCs was confirmed by qRT–PCR (Fig. 1a and Supplementary Fig. 7a). Extensive demethylation of CpG dinucleotides in the *OCT4* and *NANOG* promoters compared to their parental fibroblasts was confirmed by bisulphite sequencing (Fig. 1b).

[1]Department of Gene and Cell Medicine, Department of Developmental and Regenerative Biology, Black Family Stem Cell Institute, Mount Sinai School of Medicine, New York, New York 10029, USA. [2]Department of Regenerative Cardiology, Centro Nacional de Investigaciones Cardiovasculares, 28029 Madrid, Spain. [3]Department of Medicine, Cardiovascular Institute, Mount Sinai School of Medicine, New York, New York 10029, USA. [4]Department of Neurology, Mount Sinai School of Medicine, New York, New York 10029, USA. [5]Department of Genetics and Genomic Sciences, Mount Sinai School of Medicine, New York, New York 10029, USA. [6]Child Health and Development Institute, Mount Sinai School of Medicine, New York, New York 10029, USA. [7]Department of Medical Genetics, University Medical Center Utrecht, 3584 EA Utrecht, the Netherlands. [8]Dipartimento di Ematologia, Oncologia e Medicina Molecolare, Istituto Superiore di Sanità, 00161 Rome, Italy. [9]Department of Pediatrics, Mount Sinai School of Medicine, New York, New York 10029, USA. *These authors contributed equally to this work.

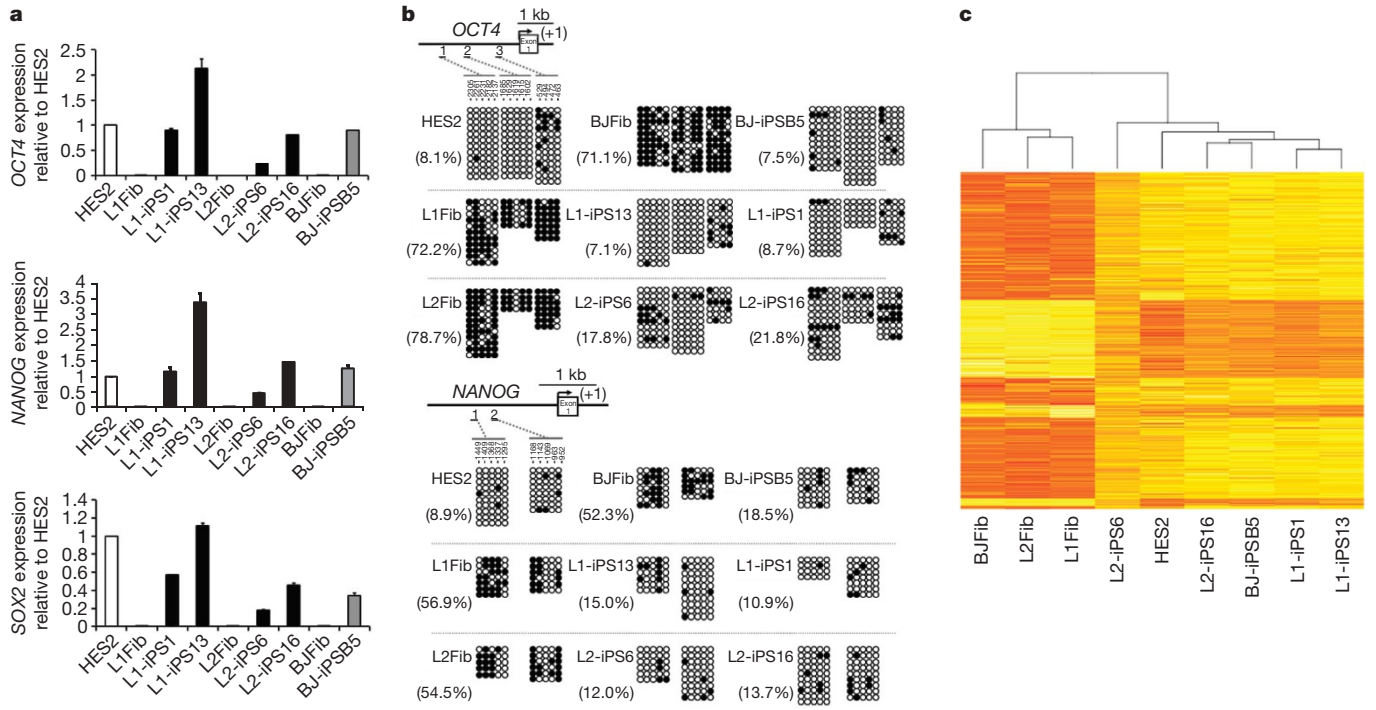

Figure 1 | Gene expression profile in LEOPARD syndrome iPSCs is similar to human ES cells. a, Quantitative real-time PCR assay for the expression of endogenous human *OCT4*, *NANOG* and *SOX2* in iPSCs and parental fibroblasts (Fib). PCR reactions were normalized against β-actin and plotted relative to expression levels in HES2. Error bars indicate ±s.d. of triplicates. **b**, Bisulphite sequencing analyses of the *OCT4* and *NANOG* promoters. The cell line and the percentage of methylation are indicated to the left of each cluster. **c**, Heat map showing hierarchical clustering of 3,657 genes with at least twofold expression change between the average of the three fibroblast cell lines versus all the iPSC lines/human ES cell samples. Expression levels are represented by colour; red indicates lower and yellow higher expression.

We next examined genome-wide messenger RNA expression profiles of two LEOPARD syndrome iPSC lines from each patient, the BJ-iPSB5 cell line, parental fibroblasts and HES2 cells. The resulting heat map and scatter-plot analyses indicated that iPSC lines shared a higher degree of similarity with HES2 cells than with their parental fibroblast cell lines (Fig. 1c and Supplementary Fig. 7b).

Pluripotent human ES cells can differentiate into cell types representative of all three germ layers. We tested the differentiation abilities of our iPSCs using an *in vitro* floating embryoid body (EB) system, followed by replating on gelatin-coated dishes[10,15]. Immunocytochemistry analyses detected expression of α-smooth muscle actin (α-SMA, mesoderm), desmin (mesoderm), α-fetoprotein (AFP, endoderm), vimentin (mesoderm), glia fibrillary acidic protein (GFAP, ectoderm) and βIII-tubulin (ectoderm) markers (Fig. 2a and Supplementary Fig. 8). To determine pluripotency *in vivo*, we injected LEOPARD syndrome iPSCs, BJ-iPSB5 and HES2 cells into

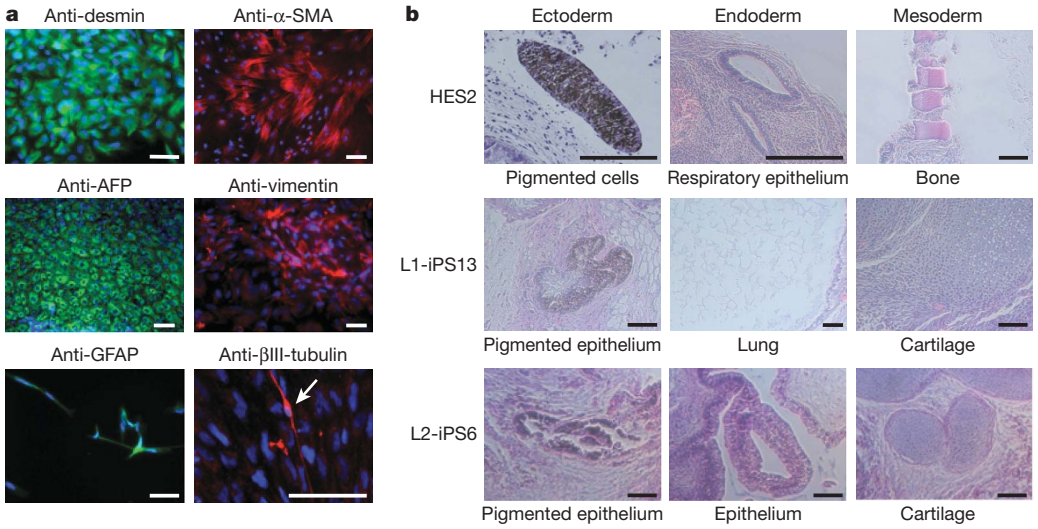

Figure 2 | LEOPARD syndrome iPSCs differentiate *in vitro* and *in vivo* into all three germ layers. a, L2-iPS6 cells were differentiated as floating EBs for 8 days and then plated onto gelatin-coated dishes and allowed to differentiate for another 8 days. Immunocytochemistry showed cell types positively stained for differentiation markers including desmin/α-SMA (mesoderm), AFP (endoderm), vimentin (mesoderm) and GFAP/βIII-tubulin (ectoderm). The arrow indicates a βIII-tubulin-positive cell. Scale bar, 100 μm. **b**, HES2, L1-iPSC and L2-iPSC were injected subcutaneously into the right hind leg of immuno-compromised NOD-SCID mice. The resulting teratomas were stained with haematoxylin and eosin and tissues representative of all three germ layers were observed. Scale bar, 100 μm.

immuno-compromised NOD-SCID mice. Histological analyses of the resulting teratomas showed cell types representative of the three germ layers, including pigmented cells (ectoderm), lung, respiratory and gut-like epithelia (endoderm), and mesenchyme, adipose tissue and cartilage (mesoderm) (Fig. 2b and data not shown).

As mentioned previously, hypertrophic cardiomyopathy is one of the major features of LEOPARD syndrome, affecting 80% of the patients. In addition, affected individuals occasionally manifest haematological complications such as myelodysplasia and leukaemia[16,17]. Therefore, we asked if LEOPARD syndrome iPSCs were able to differentiate into haematopoietic and cardiac lineages. iPSCs from both patients differentiated into a variety of haematopoietic cell types including early haematopoietic progenitors ($CD41^+$)[18], early erythroblasts ($CD71^+$/$CD235a^+$)[19] and macrophages ($CD11b^+$)[20] (Supplementary Fig. 9 and data not shown). The cardiac hypertrophic response includes induction of immediate-early genes (such as *JUN*, *FOS* and *MYC*), an increase in cell size, and organization of contractile proteins into sarcomeric units[21,22]. To have an appropriate control cell line to analyse some of these parameters, besides human ES cells, we generated a wild-type iPSC line (S3-iPS4) from fibroblasts obtained from an unaffected brother of L1 without the T468M mutation (Supplementary Figs 10 and 11). Using a well-established cardiac differentiation protocol[23], we observed contracting EBs emerging around day 11 of differentiation (Supplementary Movies 1–7). To monitor cardiac development, we analysed cardiac troponin T (cTNT) expression on day 18 of differentiation by flow cytometry (data not shown). Replated cells from beating EBs were processed as described in Methods. Briefly, cells were fixed, immunostained for cTNT (Fig. 3b) and 50 cardiomyocytes were randomly chosen from each sample for surface area measurement using a computerized morphometric system (ImageJ software, NIH). Cardiomyocytes derived from LEOPARD syndrome iPSC lines L1-iPS13, L1-iPS6 and L2-iPS10 (Supplementary Fig. 10 and Supplementary Fig. 11) had a significantly increased median surface area compared to wild-type iPSC cardiomyocytes (1.8 times, 2.5 times and 4.8 times larger, respectively), whereas the area median of the cardiomyocytes obtained from human ES cells was similar to wild-type iPSC cardiomyocytes (Fig. 3a). We also observed increased sarcomere assembly in L1-iPS6 and L2-iPS10 cells when compared to wild-type S3-iPS4 cells (Fig. 3b). Recently, the calcineurin–NFAT pathway has been shown to be an important regulator of cardiac hypertrophy. Active calcineurin dephosphorylates NFAT transcription factors, resulting in their nuclear translocation[22,24]. We analysed the localization of NFATC4 using immunocytochemistry in 50 cTNT-positive cardiomyocytes derived from the L2-iPS10 cell line, which produced the largest cardiomyocytes, and wild-type S3-iPS4. We observed a significantly higher proportion of LEOPARD syndrome cardiomyocytes with nuclear NFATC4 (~80% versus ~30%, respectively; Fig. 3c, d).

To identify potential molecular targets that could be affected by the T468M *PTPN11* mutation, protein extracts from LEOPARD syndrome iPSCs, wild-type BJ-iPSB5 and HES2 cells were analysed using a phosphoproteomic microarray chip containing approximately 600 pan and phospho-specific antibodies (Kinexus Bioinformatics Corporation). We established eight groups for comparison, each of the LEOPARD syndrome iPSC lines versus one control cell line, either HES2 or wild-type iPSCs. Proteins with a 1.5-fold change were filtered, and those that were conserved in most of the groups were represented in a heat map (Fig. 4a). Some of the proteins were more abundantly present in LEOPARD syndrome iPSCs when compared to either HES2 cells (DDR2, TYK2 and haspin) or wild-type iPSCs (p-MARCKs, p-synapsin 1, p-GRIN2B, p-RPS6KA5, p-RSK1/3 and p-p53). The phosphorylation of other proteins was increased (p-caveolin 2, p-MEK1, p-EGFR and p-FAK) or decreased (p-vinculin, p-S6 and p-LCK) in LEOPARD syndrome iPSCs when compared to control cell lines. To eliminate false positives, we verified the phosphoproteomic results by western blot for three of the most altered proteins (p-S6, p-EGFR and p-MEK1) in four LEOPARD syndrome

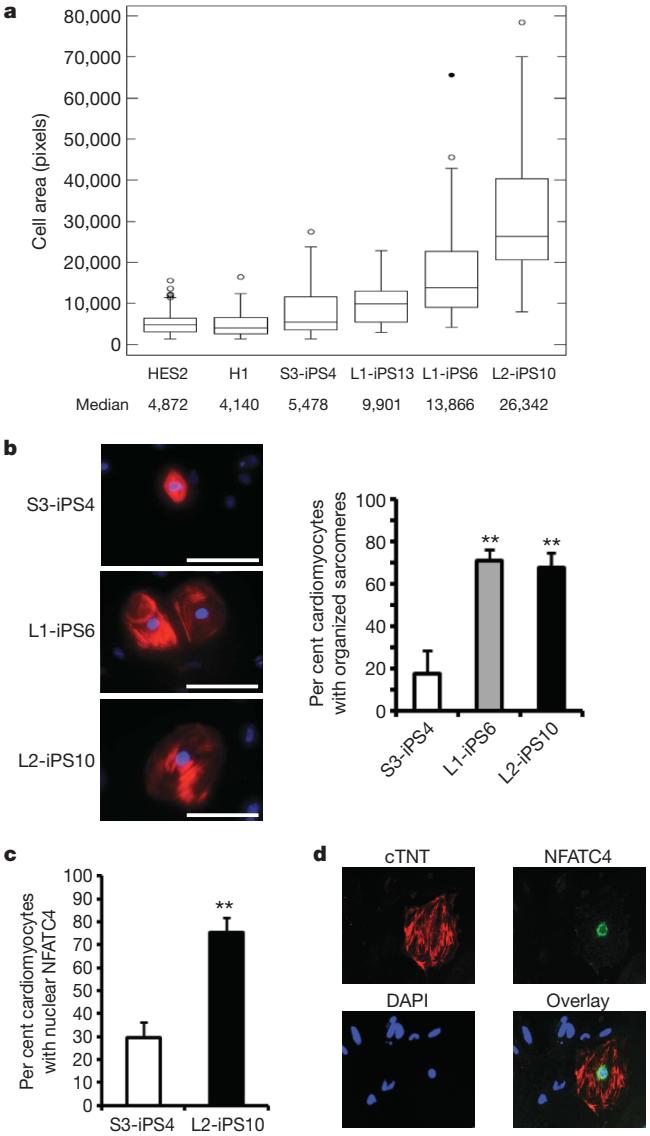

Figure 3 | Cardiomyocytes derived from LEOPARD syndrome iPSCs show hypertrophic features. a, HES2, H1, wild-type S3-iPS4 and three LEOPARD syndrome iPSC clones were differentiated into cardiac lineage. Cell areas of 50 random cTNT-positive cardiomyocytes of each cell line were measured using ImageJ. Boxes show the span from the median (50th percentile) to the first and third quartiles. The lines represent the largest/smallest sizes that are no more than 1.5 times the median to quartile distance. Additional points drawn represent extreme values, ≥1.5 times (open circles) and ≥3 times (filled circle) the median to quartile distance. **b**, Sarcomeric organization was assessed in 50 cTNT-positive (red) cardiomyocytes. Data are presented as mean ± s.d. $n = 3$; $^{**}P < 0.01$ (Student's *t*-test). **c**, S3-iPS4 and L2-iPS10 cell-derived cardiomyocytes were re-stained with NFATC4 antibody, and the nuclear versus cytosolic expression was analysed. $n = 3$; $^{**}P < 0.01$ (Student's *t*-test). **d**, Nuclear localization of NFATC4 protein in a cTNT-positive cell from L2-iPS10 is shown.

iPSC lines, in comparison to wild-type iPSCs. Although we did not confirm a major change in the phosphorylation status of S6 protein (data not shown), western blot confirmed that the phosphorylation of EGFR and MEK1 proteins was considerably increased in the LEOPARD syndrome iPSC samples (Fig. 4b).

RAS–mitogen-activated protein kinase (MAPK) represents the major signalling pathway deregulated by SHP2 mutants. Noonan syndrome mutants increase basal and stimulated phosphatase activity, whereas LEOPARD syndrome mutants are catalytically impaired and have dominant-negative effects, inhibiting growth-factor-evoked ERK1/2 activation[25]. We analysed the ability of LEOPARD syndrome

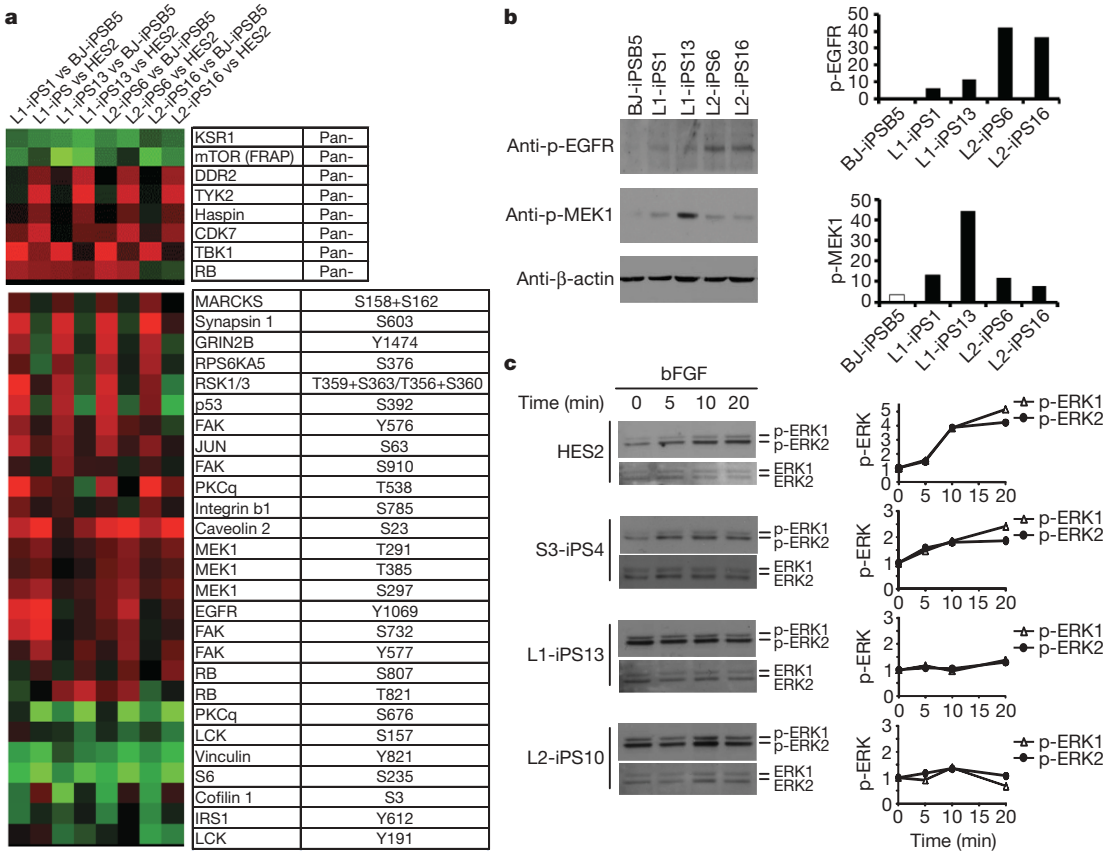

Figure 4 | Phosphoproteomic and MAPK activation analyses. **a**, Protein extracts of two iPSCs from each LEOPARD syndrome patient (L1 and L2), wild-type iPSCs (BJ-iPSB5) and HES2 cells were hybridized to an antibody microarray. The heat map represents the most significant protein changes preserved in all the comparison groups. **b**, p-MEK1 and p-EGFR expression was confirmed by western blot using phospho-specific antibodies. Band density was measured (ImageJ software) and normalized to β-actin. **c**, HES2, wild-type S3-iPS4 and LEOPARD syndrome iPSCs were serum- and bFGF-starved for 6 h and then treated with bFGF (20 ng ml^{-1}) for the indicated time. Phosphorylated ERK1/2 (p-ERK1/2) and total ERK were assessed by immunoblotting and quantified. p-ERK1/2 levels were compared to the untreated p-ERK1/2 level in each sample, normalized to the total ERK1/2 and represented graphically at the right of each panel.

iPSCs to respond to external growth factors. We used basic fibroblast growth factor (bFGF), the main growth factor in the maintenance of human ES cells, to induce the stimulation of the MAPK signalling pathway. bFGF treatment increased the phosphorylation of ERK1/2 (p-ERK) levels over time in HES2 and wild-type S3-iPS4 cells (Fig. 4c). Although the LEOPARD syndrome iPSCs expressed the four FGF receptor (FGFR) family members (Supplementary Fig. 12a), bFGF stimulation did not cause any substantial change in p-ERK levels (Fig. 4c and Supplementary Fig. 12b, c). However, the LEOPARD syndrome iPSC lines had higher basal p-ERK levels compared to HES2 and S3-iPS4 cells (Fig. 4c and Supplementary Fig. 12b, c), in accordance with the increased p-MEK1—the upstream kinase of ERK—levels found in LEOPARD syndrome iPSC samples in phosphoproteomic array results.

We have generated and characterized LEOPARD syndrome patient-specific iPSCs, providing a new system for the study of disease pathogenesis. Some of the standard procedures to analyse cardiomyocyte hypertrophy (for example, protein synthesis rate, re-activation of the fetal gene program) could not be reliably assessed due to the variably mixed population of cells obtained using this cardiac differentiation procedure (for example, endothelial, cardiomyocytes), and the lack of a reliable cell surface marker for cardiomyocyte purification. However, we observed increases in cell size, sarcomeric organization and nuclear NFATC4 localization in LEOPARD syndrome iPSC-derived cardiomyocytes, when compared to human ES cell and wild-type iPSC-derived cardiomyocytes. These results would be consistent with cardiac hypertrophy, a condition commonly found in LEOPARD syndrome patients[2], and indicate that this abnormality occurs through a cell-autonomous mechanism due to the *PTPN11* mutation. Because many human cell types, such as cardiomyocytes, cannot be propagated readily in cell culture, iPSC-derived cells exhibiting disease-relevant phenotypes provide the requisite resource for precisely elucidating pathogenesis and pursuing novel therapeutic strategies.

In our studies, we also attempted to provide insights into the molecular events that could be affected by the *PTPN11* mutation in the pluripotent iPSCs using antibody microarrays. We found that the phosphorylation of certain proteins was increased in LEOPARD syndrome iPSCs when compared to wild-type human ES cells and iPSCs. Further analysis will be required to elucidate if these proteins/signalling pathways are involved in the development of the disease phenotype. Notably, one of the more upregulated phosphoproteins was MEK1, the upstream kinase of ERK1/2, the gene of which is sometimes mutated in the related disorder cardiofaciocutaneous syndrome. *PTPN11* mutations underlie 45% and 90% of Noonan syndrome and LEOPARD syndrome, respectively. It is not well understood how mutations that provoke opposite effects on SHP2 phosphatase activity cause syndromes with similar features[26]. In concordance with observations in the *Drosophila* LEOPARD syndrome model[7], basal p-ERK levels were increased in LEOPARD syndrome iPSCs. Of note, receptor tyrosine kinase stimulation with bFGF in LEOPARD syndrome iPSCs failed to elicit further activation of ERK, as previously observed in a different cellular model[25]. This result demonstrates that RAS–MAPK signal transduction is perturbed in LEOPARD syndrome as early as the pluripotent stem-cell stage. Taken together, this is, to our knowledge, the first described human model of an inherited RAS pathway disorder.

METHODS SUMMARY

Cell culture. Dermal fibroblast lines were obtained from skin biopsies, collected under an Institutional Review Board-approved protocol and with informed consent. Fibroblasts and GP2 cells were maintained in Dulbecco's modified Eagle medium (DMEM) containing 10% fetal bovine serum and penicillin/streptomycin (Invitrogen). HES2 cells and iPSCs were maintained on irradiated Swiss–Webster mouse embryonic feeder cells (MEFs), in a serum-free human ES cell medium containing 20 ng ml^{-1} bFGF (R&D Systems).

LEOPARD syndrome iPSC generation. *OCT4*, *SOX2*, *KLF4* and *MYC* transcription factors were introduced in dermal fibroblasts derived from two patients with LEOPARD syndrome via the pMXs retroviral vector. In parallel, the pMXs-EGFP vector was used to estimate the infection efficiency (data not shown). Six days after infection, fibroblasts were seeded onto MEFs. The following day the medium was replaced with the human ES cell medium and bFGF.

Microarray analysis. Gene-level mRNA abundance measures were extracted using the Affymetrix GeneChip Exon 1.0 ST array, and Robust Multi-Array (RMA)-normalized using the Affymetrix Expression Console software. Subsequently, these genes were clustered and a heat map was generated against a background subset of genes showing at least twofold change between sample averages of iPSC/HES2 cells and fibroblast samples.

***In vitro* differentiation.** For non-lineage-specific and haematopoietic differentiation we used previously described protocols[10,15,27], with certain modifications[28]. For cardiomyocyte induction, we used a well-established assay[23].

Phosphoproteomics. HES2 cells and iPSCs were incubated overnight in human ES cell culture medium deprived of bFGF and knockout serum replacement (KSR). Protein lysates were quantified by Bradford assay and sent to Kinexus Bioinformatics Corporation for antibody microarray screening. The proteins with at least 1.5-fold change between the LEOPARD syndrome iPSC samples and control sample (either HES2 or wt-iPSC), and conserved in the majority of the comparison groups, were represented in a heat map.

Full Methods and any associated references are available in the online version of the paper at www.nature.com/nature.

Received 16 December 2009; accepted 8 March 2010.

1. Gorlin, R. J., Anderson, R. C. & Moller, J. H. The Leopard (multiple lentigines) syndrome revisited. *Birth Defects Orig. Artic. Ser.* **7,** 110–115 (1971).
2. Sarkozy, A., Digilio, M. C. & Dallapiccola, B. Leopard syndrome. *Orphanet J. Rare Dis.* **3,** 13 (2008).
3. Loh, M. L. *et al.* Mutations in PTPN11 implicate the SHP-2 phosphatase in leukemogenesis. *Blood* **103,** 2325–2331 (2004).
4. Tartaglia, M. *et al.* Genetic evidence for lineage-related and differentiation stage-related contribution of somatic PTPN11 mutations to leukemogenesis in childhood acute leukemia. *Blood* **104,** 307–313 (2004).
5. Tartaglia, M. *et al.* Diversity and functional consequences of germline and somatic PTPN11 mutations in human disease. *Am. J. Hum. Genet.* **78,** 279–290 (2006).
6. Jopling, C., van Geemen, D. & den Hertog, J. Shp2 knockdown and Noonan/LEOPARD mutant Shp2-induced gastrulation defects. *PLoS Genet.* **3,** e225 (2007).
7. Oishi, K. *et al.* Phosphatase-defective LEOPARD syndrome mutations in PTPN11 have gain-of-function effects during Drosophila development. *Hum. Mol. Genet.* **18,** 193–201 (2008).
8. Lowry, W. E. *et al.* Generation of human induced pluripotent stem cells from dermal fibroblasts. *Proc. Natl Acad. Sci. USA* **105,** 2883–2888 (2008).
9. Park, I. H. *et al.* Disease-specific induced pluripotent stem cells. *Cell* **134,** 877–886 (2008).
10. Takahashi, K. *et al.* Induction of pluripotent stem cells from adult human fibroblasts by defined factors. *Cell* **131,** 861–872 (2007).
11. Ebert, A. D. *et al.* Induced pluripotent stem cells from a spinal muscular atrophy patient. *Nature* **457,** 277–280 (2009).
12. Lee, G. *et al.* Modelling pathogenesis and treatment of familial dysautonomia using patient-specific iPSCs. *Nature* **461,** 402–406 (2009).
13. Raya, A. *et al.* Disease-corrected haematopoietic progenitors from Fanconi anaemia induced pluripotent stem cells. *Nature* **460,** 53–59 (2009).
14. Ye, Z. *et al.* Human induced pluripotent stem cells from blood cells of healthy donors and patients with acquired blood disorders. *Blood* **114,** 5473–5480 (2009).
15. Dimos, J. T. *et al.* Induced pluripotent stem cells generated from patients with ALS can be differentiated into motor neurons. *Science* **321,** 1218–1221 (2008).
16. Laux, D., Kratz, C. & Sauerbrey, A. Common acute lymphoblastic leukemia in a girl with genetically confirmed LEOPARD syndrome. *J. Pediatr. Hematol. Oncol.* **30,** 602–604 (2008).
17. Ucar, C., Calyskan, U., Martini, S. & Heinritz, W. Acute myelomonocytic leukemia in a boy with LEOPARD syndrome (*PTPN11* gene mutation positive). *J. Pediatr. Hematol. Oncol.* **28,** 123–125 (2006).
18. Mikkola, H. K., Fujiwara, Y., Schlaeger, T. M., Traver, D. & Orkin, S. H. Expression of CD41 marks the initiation of definitive hematopoiesis in the mouse embryo. *Blood* **101,** 508–516 (2003).
19. Wu, C. J. *et al.* Evidence for ineffective erythropoiesis in severe sickle cell disease. *Blood* **106,** 3639–3645 (2005).
20. Fan, S. T. & Edgington, T. S. Coupling of the adhesive receptor CD11b/CD18 to functional enhancement of effector macrophage tissue factor response. *J. Clin. Invest.* **87,** 50–57 (1991).
21. Aoki, H., Sadoshima, J. & Izumo, S. Myosin light chain kinase mediates sarcomere organization during cardiac hypertrophy *in vitro*. *Nature Med.* **6,** 183–188 (2000).
22. Buitrago, M. *et al.* The transcriptional repressor Nab1 is a specific regulator of pathological cardiac hypertrophy. *Nature Med.* **11,** 837–844 (2005).
23. Yang, L. *et al.* Human cardiovascular progenitor cells develop from a KDR^{+} embryonic-stem-cell-derived population. *Nature* **453,** 524–528 (2008).
24. Molkentin, J. D. Calcineurin-NFAT signaling regulates the cardiac hypertrophic response in coordination with the MAPKs. *Cardiovasc. Res.* **63,** 467–475 (2004).
25. Kontaridis, M. I., Swanson, K. D., David, F. S., Barford, D. & Neel, B. G. PTPN11 (Shp2) mutations in LEOPARD syndrome have dominant negative, not activating, effects. *J. Biol. Chem.* **281,** 6785–6792 (2006).
26. Edouard, T. *et al.* How do Shp2 mutations that oppositely influence its biochemical activity result in syndromes with overlapping symptoms? *Cell. Mol. Life Sci.* **64,** 1585–1590 (2007).
27. Kennedy, M., D'Souza, S. L., Lynch-Kattman, M., Schwantz, S. & Keller, G. Development of the hemangioblast defines the onset of hematopoiesis in human ES cell differentiation cultures. *Blood* **109,** 2679–2687 (2007).
28. Grigoriadis, A. E. *et al.* Directed differentiation of hematopoietic precursors and functional osteoclasts from human ES and iPS cells. *Blood* **115,** 2769–2776 (2010).

Supplementary Information is linked to the online version of the paper at www.nature.com/nature.

Acknowledgements We thank T. James, X. Niu and D. York for their technical support and laboratory management, and B. MacArthur for support in microarray analysis. We also would like to thank K. Moore and her laboratory, and S. Mulero-Navarro from B.D.G.'s laboratory for their help, and V. Fuster and A. Bernad for their support. This research was funded by grants from the National Institutes of Health (NIH) to I.R.L (5R01GM078465), the Empire State Stem Cell Fund through New York State Department of Health (NYSTEM) C024410 to I.R.L. and C.S., C024176 (HESC-SRF) to I.R.L. and S.L.D., C024407 to B.D.G., American College of Cardiology/Pfizer Research Fellowship to E.D.A., and ERA-Net for research programmes on rare diseases 2009 to M.T. X.C.-V. is a recipient of a Postdoctoral Fellowship from the Ministerio de Ciencia e Innovacion/Instituto de Salud Carlos III, D.-F.L. is a New York Stem Cell Foundation Stanley and Fiona Druckenmiller Fellow and S.P. is a recipient of a Ruth L. Kirschstein National Research Service Award (NRSA) Institutional Research Training Grant (T32).

Author Contributions X.C.-V. (iPSC establishment, project planning, experimental work and preparation of manuscript); A.S., S.L.D., Y.-S.A., L.Y., A.D.K., E.D.A., D.-F.L., A.W., B.C., J.S. and S.P. (experimental work); R.R. and Y.G. (microarray analysis); N.C. and L.J.E. (karyotype analysis); K.D.L. and M.T. (obtaining of fibroblast samples from patients); C.S. (project planning, experimental work); B.D.G. and I.R.L. (project planning, preparation of manuscript).

Author Information Microarray data have been deposited in NCBI-GEO under the accession number GSE20473. Reprints and permissions information is available at www.nature.com/reprints. The authors declare no competing financial interests. Correspondence and requests for materials should be addressed to I.R.L. (ihor.lemischka@mssm.edu) or X.C.-V. (xcarvajal@gmail.com).

METHODS

Cell culture. Fibroblasts derived from LEOPARD syndrome patients, BJ fibroblasts (American Type Culture Collection) and GP-2 cells were maintained in DMEM 10% FBS medium. iPSCs and human ES cells were maintained on mitotically inactivated MEFs in human ES cell medium composed of DMEM/F12 (Cellgro, Mediatech) containing 20% (vol/vol) KSR (Invitrogen), 5% (vol/vol) MEF-conditioned medium, penicillin/streptomycin, L-glutamine (L-Gln), non-essential amino acids (Invitrogen), β-mercaptoethanol (β-ME, Sigma-Aldrich) and bFGF (R&D Systems).

Plasmid construction. Full-length sequences of human *OCT4*, *SOX2*, *KLF4* and *MYC* transcription factors were obtained from Open Biosystems. The coding sequences were PCR amplified using Pfu Turbo (Stratagene) and cloned into pMXs vector and verified by sequencing. pMXs-EGFP vector was constructed by introducing the BamHI/NotI EGFP fragment from FUGW (provided by C. Lois) into pMXs vector. The latter vector was used to monitor the transfection and infection efficiency. Detailed primer and cloning information will be provided upon request.

Retroviral infection and human iPSC generation. GP-2 cells were plated at 8×10^6 cells per 10-cm dish and transfected with pMXs, VSV-G and Gag-Pol vectors using SuperFect transfection reagent on the following day. The same day, human fibroblasts were seeded at 8×10^5 cells per 10-cm dish. Twenty-four hours after transfection, the four retroviruses (*OCT4*, *SOX2*, *KLF4* and *MYC*) containing supernatants were collected, and equal amounts of each were mixed and filtered through a 0.45-μm pore-size filter, and supplemented with 4 μg ml^{-1} polybrene. Retrovirus-containing medium was added to the fibroblasts plates. The following day, 48-h after transfection, the fibroblasts were re-infected following the same procedure as the day before. Six days after transduction, fibroblasts were transferred into four dishes coated with MEFs, at 50,000 fibroblasts per plate.

DNA fingerprinting analysis. To verify the genetic relatedness of the iPSCs to their parental fibroblasts, we PCR amplified across three discrete genomic loci containing highly variable numbers of tandem repeats. Genomic DNA (gDNA) was isolated with the Easy-DNA kit (Invitrogen). Fifty nanograms of genomic DNA was used per reaction. Primers are summarized in Supplementary Table 1.

Karyotype analysis. HES2 cells and iPSCs were grown on Matrigel-coated glass coverslip dishes (MatTek, Ma). The day of culture harvest, 20 μl of colcemid (5 μg ml^{-1}) was added to the *in situ* ESCl culture which was 30–50% confluent. The culture was re-incubated for 15 min at 37 °C. A robotic harvester (Tecan) was used, which included automatic addition of 2 ml of hypotonic solution (sodium citrate solution 0.8%) with incubation for 20 min at 25 °C, pre-fixation with addition of 2 ml of fixative (methanol: glacial acetic acid; 3:1), followed by addition of 4cc of fixative, twice. The coverslip was dried completely at 37 °C with 45–50% humidity and mounted on a microscope slide and GTG-banded according to standard protocols. Metaphases were captured and karyotypes were prepared using the CytoVision software program (Version 3.92 Build 7, Applied Imaging).

qPCR and transgene integration. For quantitative real-time PCR (qPCR) analyses, total RNA was extracted from cells using Trizol Reagent (Invitrogen) and subsequently column-purified with the RNeasy kit (Qiagen) and treated with RNase-free DNase (Qiagen). One microgram of total RNA was reverse transcribed into cDNA using random primers and Superscript II Reverse Transcriptase (Invitrogen). PCR for transgene silencing was performed with Expand High Fidelity Enzyme Taq Polymerase (Roche). Real-time qPCR was performed on a StepOne Plus Real-Time PCR System (Applied Biosystems) with Fast SYBR Green Master Mix (Applied Biosystems). The results were analysed with the StepOne Software v2.0, normalized to β-actin gene expression, and compared to HES2 cell expression levels. To examine the presence of transgenes in the iPSC lines, gDNA was isolated with the Easy-DNA Kit (Invitrogen). PCR reactions were carried out with the Expand High Fidelity Enzyme Taq Polymerase (Roche). Primer sequences are described in Supplementary Table 1. Primers for FGF receptors expression analysis have been previously described[29].

Southern blot analyses. gDNA (2 μg) was completely digested with BglII, separated on a 0.8% agarose gel, transferred to a positively charged nylon membrane, and hybridized with DIG-labelled human *OCT4*, *SOX2*, *KLF4* and *MYC* cDNA probes. After hybridization, membranes were washed, blocked with DIG blocking solution, and incubated with anti-DIG-AP Fab fragments (Roche). Probe-target hybrids were then incubated with chemiluminescent CDP-Star substrates (Roche) and detected via exposure to X-ray film.

Bisulphite sequencing. We treated 500 ng of purified gDNA with sodium bisulphite using the Zymo EZ-DNA Methylation Kit, following the manufacturer's instructions. The sequences of primers used for amplification of genomic fragments were previously published[30]. PCR products were then size fractionated in 1% TAE-agarose, extracted using the Qiaquick gel extraction kit (Qiagen) and cloned into the pGEM-T Easy Vector system (Promega). Blue-white selection was applied to eliminate false positives, and 12 random clones were picked and sequenced. Bisulphite conversion efficiency of non-CpG cytosines was >90% for all individual clones for each sample.

Immunocytochemistry, AP staining and FACS analysis. For *in vivo* immunostaining, HES2 cells and iPSCs were washed once with DMEM medium supplemented with 10% FBS and antibiotics (DMEM 10%), and incubated with biotin-TRA1-81 antibody (1:100, eBiosciences) for 2 h. Cells were washed three times with DMEM 10% and they were incubated with the secondary antibody streptavidin-FITC (1:100, eBiosciences) and the phycoerythrin TRA1-60 (PE-TRA1-60) antibody (1:100, eBiosciences) where indicated. All the incubations were performed in a humidified incubator at 37 °C with 5% CO_2. For intracellular staining, cells were fixed in 2% paraformaldehyde for 30 min, and blocked and permeabilized in PBS containing 10% donkey serum, 1% BSA and 0.1% Triton X-100 for 45 min. Cells were incubated with primary antibody in blocking solution overnight at 4 °C, washed and incubated with the corresponding Alexa donkey secondary antibody for 1 h at 25 °C. Then cells were washed and stained with DAPI (1 μg ml^{-1}) for 20 min. The primary antibodies used for intracellular immunostaining were OCT4 (1:100, BioVision), NANOG (1:100, R&D Systems), desmin (1:100, Lab Vision), α-SMA (pre-diluted, DAKO), vimentin (1:100, Chemicon), AFP (1:500, DAKO), GFAP (1:1000, DAKO), βIII-tubulin (1:100, Chemicon), or NFATC4 (1:100, Santa Cruz Biotechnology). All the secondary antibodies, Alexa 488 donkey anti-rabbit (1:100), Alexa 546 donkey anti-goat (1:100) and Alexa 546 donkey anti-mouse (1:100) were obtained from Invitrogen. Alkaline phosphatase staining was detected following the manufacturer's recommendations (Millipore). SSEA-4, troponin T and haematopoietic marker expression were evaluated on a BD Biosciences LSRII FACS machine analyser. Primary antibodies SSEA-4-PE (R&D Systems), cardiac troponin T (Lab Vision), CD11b-APC (Caltag), and CD45-APC, CD45-PE, CD71-PE, CD41-PE and CD235a-APC were purchased from BD Biosciences.

Teratoma formation. All animal procedures were performed in accordance with the Mount Sinai Medical Center's Institutional Animal Care and Use Committee. Approximately 1–2 × 10^6 cells were injected subcutaneously into the right hind leg of immuno-compromised NOD-SCID mice (The Jackson Laboratory). Teratomas were excised 6–10 weeks after injection, fixed overnight in formalin, embedded in paraffin, sectioned and stained with haematoxylin and eosin by the Morphology and Assessment Core of the Department of Gene and Cell Medicine. Histological evaluation was performed using a Nikon TE2000-U microscope and ACT-1 software.

***In vitro* differentiation.** For non-lineage-specific differentiation we used previously described protocols[10,15] with certain modifications. For EB formation, HES2 cells and iPSCs were treated with collagenase B (Roche) for 10 min, and collected by scraping. After centrifuging, cell pellets were re-suspended in basic differentiation media, StemPro 34 (Invitrogen), containing 2 mM L-Gln, 4×10^{-4} monothioglycerol (MTG), 50 μg ml^{-1} ascorbic acid (Sigma) and 150 μg ml^{-1} transferrin (Sigma). EBs were grown in ultra-low-binding plates (Costar) and medium was changed every 3 days. After 8 days of differentiation, EBs were collected, re-suspended in DMEM 10% and transferred to gelatin-coated dishes to allow them to attach and differentiate for eight additional days before processing for immunocytochemistry analyses. For haematopoietic differentiation we used a described protocol[27] with certain modifications[28]. For cardiomyocyte induction, we used a well-established protocol[23].

Microarray analysis. RNA probes were hybridized to Affymetrix GeneChip Exon 1.0ST array according to the manufacturer's protocols by the Genomics Core Lab in The Institute for Personalized Medicine at Mount Sinai Medical Center. Microarrays were scanned and data were analysed using the Affymetrix Expression Console software.

Cytology/cardiomyocyte size determination. On day 18 of differentiation, beating EBs were plated on gelatin-coated dishes. Three days after plating, EB outgrowths were trypsinized, filtered through a 40-μm size pore-size filter, and single cells were replated at low density on gelatin-coated dishes. The following day, cells were fixed with 4% paraformaldehyde, permeabilized, blocked in PBS/1% BSA/0.1% Triton/10% donkey serum, and stained for cardiac troponin T (1:200, Lab Vision) overnight at 4 °C. Stained cells were washed three times with PBS, and then incubated with the Alexa Fluor 547 donkey-anti-mouse antibody (Invitrogen) for 1 h. The areas of human ES cell- and LEOPARD syndrome iPSC-derived cardiomyocytes were analysed using ImageJ software (NIH).

Phosphoproteomics and western blotting. We prepared a lysis buffer (pH 7.2) containing 20 mM MOPS pH 7.0, 2 mM EGTA, 5 mM EDTA, 30 mM sodium fluoride, 60 mM β-glycerophosphate, 20 mM sodium phyrophospate and 1% Triton X-100. Protease and phosphatase inhibitors (1 mM phenylmethylsulphonyl fluoride, 3 mM benzamidine, 10 μg ml^{-1} aprotinin, 10 μM leupeptin, 5 μM pepstatin, 1 mM dithiothreitol and 1 mM sodium orthovanadate) were added to the lysis buffer immediately before use. Protein extracts were sent to Kinexus Bioinformatics Corporation. The antibody microarray results were processed following the company recommendations. Western blot was carried out as previously described[31]. The primary antibodies used were: pS6 S235/236 (1:1,000, Cell Signaling), pEGFR Y1086 (1:1,000, Cell Signaling), pMEK1 S298 (1:1,000, Cell

Signaling), β-actin (1:5,000, Abcam), p-ERK1/2 T202/Y204 (1:2,000 Cell Signaling) and ERK1 (1:2,500, Santa Cruz Biotechnology).

29. Dvorak, P. *et al.* Expression and potential role of fibroblast growth factor 2 and its receptors in human embryonic stem cells. *Stem Cells* **23**, 1200–1211 (2005).
30. Freberg, C. T., Dahl, J. A., Timoskainen, S. & Collas, P. Epigenetic reprogramming of OCT4 and NANOG regulatory regions by embryonal carcinoma cell extract. *Mol. Biol. Cell* **18**, 1543–1553 (2007).
31. Carvajal-Vergara, X. *et al.* Multifunctional role of Erk5 in multiple myeloma. *Blood* **105**, 4492–4499 (2005).